Mechanism of Photodimerization of Acenaphthylene

Naoki Haga,* Hiroaki Takayanagi, and Katsumi Tokumaru†

School of Pharmaceutical Sciences, Kitasato University, Minato-ku, Tokyo 108, Japan, and University of Tsukuba, Tsukuba, Ibaraki 305, Japan

Received December 30, 1996⊗

The mechanism of photodimerization of acenaphthylene (ACN) has been investigated in order to elucidate the roles of the singlet and the triplet excited states of ACN in the formation of the *Z*- and *E*-dimers in several solvents. The quantum yields and the ratio of the produced *Z*- to *E*-dimer were determined under irradiation of ACN at 435.8 nm in several solvents (1,2-dichloroethane, acetonitrile, cyclohexane, benzene, methanol, and DMF) over a wide concentration range (2.0×10^{-4}−2.0 M) in the absence of additives and in the presence of 1,2-dibromoethane, a heavy-atom-containing solvent; Eosin-Y, a triplet sensitizer (irradiated at 546.1 nm); and ferrocene, a triplet quencher. On irradiation of ACN in dilute solution, the initially generated S_1 state crosses over to the T_1 state, though with low quantum yield, before reaction with the ground state ACN can occur due to the very short lifetime of the S_1 state, and the resultant T_1 state reacts with ground state ACN to give a mixture of the *Z*- and *E*-dimers in a ratio that depends on the solvent employed. In more concentrated solution, the S_1 state reacts with ACN before intersystem crossing to the T_1 state can occur, affording exclusively the *Z*-dimer.

Over the past 3 decades, much attention has been paid to the photophysics and photochemistry of acenaphthylene (ACN), a simple nonalternant aromatic hydrocarbon, because of its characteristic features.[1−6] ACN shows very weak fluorescence both from the S_1 state[2−5] and the S_2 state[5] and has an extremely low intersystem crossing efficiency (Φ_{ST}: 0.00 ± 0.02 in toluene)[6] in contrast to its dihydrogenated product, acenaphthene, which has high values of Φ_F (0.50)[7] and Φ_{ST} (0.46).[7] The major deactivation pathway of the S_1 state is an efficient $S_1 \rightarrow S_0$ internal conversion, due to a configurational change of the ACN molecule after excitation to the S_1 state.[5] Distortion in this state would lead to a large Frank−Condon overlap with higher vibrational levels of the S_0 state, resulting in rapid nonradiative decay from the S_1 state to the S_0 state with a very short lifetime (e.g., 3.54 ps in cyclohexane).[5] Also, ACN does not phosphoresce at low temperature.[8]

Because of the short lifetime of the singlet state and the very low Φ_{ST} value, ACN is expected to be photochemically inactive in both the singlet and the triplet states. However, the carbon−carbon double bond of ACN does participate in some photochemical addition reactions resembling those of usual alkenes.[4,9−15] Eighty years ago, Dziewonski et al. discovered that, when exposed to sunlight, ACN is converted into two isomeric dimers (the *Z*- and *E*-dimers).[9−11] Since then, this reaction has attracted further attention because of its complex mechanism.[12,13,15−20] Livingston and Wei[17] irradiated ACN at various concentrations in methanol and benzene (0.05−1.5 M) and found that both quantum yields and chemical yields of the *Z*-dimer in degassed solutions increase with increase of [ACN], based on determination of ACN and the resultant dimers by UV spectroscopy. Only the *Z*-dimer was found in oxygen-saturated solutions. They determined the apparent molecular weight of ACN in *n*-hexane as 154 using a differential vapor pressure method, i.e., slightly higher than the formula weight, 152. On this basis, they proposed that two ACN molecules in the ground state interact weakly in a face-to-face manner and the excitation of this "van der Waals dimer" exclusively gives the *Z*-dimer via a unimolecular reaction of the excited "dimer", whereas excitation of the monomer affords both the *Z*- and *E*-dimer.

Cowan and Drisco[19,20] conducted the photodimerization in concentrated solution (higher than 0.3 M) and found that the relative quantum yield of the dimerization and the *Z*/*E* ratio increased linearly with increase of [ACN] by means of gravimetric determination of ACN and the dimers. Under sensitization, they obtained the *E*-dimer as the major product.[20,21] Ferrocene and oxygen quenched the formation of the *E*-dimer but only slightly reduced that of the *Z*-dimer.[20] Heavy-atom-containing solvents such as iodoethane and 1-bromopropane increased the yield of the *E*-dimer.[22−25] The relative yield of the *E*-dimer was correlated with the square of the spin−

† University of Tsukuba.

⊗ Abstract published in *Advance ACS Abstracts,* May 1, 1997.

(1) Heilbronner, E.; Weber, J. P.; Michl, J; Zahradnik, R. *Theor. Chim. Acta* **1966**, *6*, 141.
(2) Brown, E. J. *Advances in Photochemistry*; Vol. 1; John Wiley and Sons: New York, 1963; pp 23−42.
(3) Plummer, B. F.; Hopkinson, M. J.; Zoeller, J. K. *J. Am. Chem. Soc.* **1979**, *101*, 6779.
(4) Castellan, G.; Dumartin, G.; Bouas-Laurent, H. *Tetrahedron* **1980**, *36*, 97−103.
(5) Samanta, A.; Devadoss, C.; Fessenden, R. W. *J. Phys. Chem.* **1990**, *94*, 7106−7110.
(6) Dunsbach, R.; Schmidt, R. *J. Photochem. Photobiol. A: Chem.* **1994**, *83*, 7−13.
(7) Murov, S. L.; Carmichael, I.; Hug, G. L. *Handbook of Photochemistry*, 2nd ed.; Marcel Decker, Inc.: New York, 1993; pp 4.
(8) Ferree, Jr., W. I.; Plummer, B. F. *J. Am. Chem. Soc.* **1973**, *95*, 6709.
(9) Dziewonski, K.; Rapalski, G. *Chem. Ber.* **1912**, *45*, 2491.
(10) Dziewonski, K.; Paschalski, C. *Chem. Ber.* **1913**, *46*, 1986.
(11) Dziewonski, K.; Leyko, Z. *Chem. Ber.* **1914**, *47*, 1679.
(12) Bowen, E. J.; Marsh, J. D. F. *J. Chem. Soc.* **1947**, 109−110.
(13) Devidson, R. S. *J. Chem. Soc. Chem. Commun.* **1969**, 1450−1451.
(14) Shirota, Y.; Nagata, J.; Mikawa, H. *Chem. Lett.* **1972**, 49−50.
(15) Plummer, B. F.; Hall, R. A. *J. Chem. Soc. Chem. Commun.* **1970**, 44−45.
(16) Griffin, G. W.; Veber, D. F. *J. Am. Chem. Soc.* **1960**, *82*, 6467.
(17) Livingston, R.; Wei, K. S. *J. Phys. Chem.* **1967**, *71*, 541−547.
(18) Hartmann, I.; Hartmann, W. Schenck, G. O. *Chem. Ber.* **1967**, *100*, 3146.
(19) Cowan, D. O.; Drisco, R. L. *Tetrahedron Lett.* **1967**, 1255−1258.
(20) Cowan, D. O.; Drisco, R. L. *J. Am. Chem. Soc.* **1970**, *92*, 6286−6291.
(21) White, E. H.; Wildes, P. D.; Wiecko, J.; Doshan, H.; Wei, C. C. *J. Am. Chem. Soc.* **1973**, *95*, 7050−7058.

S0022-3263(96)02397-3 CCC: $14.00

orbit coupling parameter of the heavy atom in these solvents.[22,24]

On the basis of the studies by Livingston and Wei[17] and by Cowan and co-workers,[19,20,22−24] it has been concluded that on direct irradiation of ACN the *E*-dimer is formed from the triplet (T_1) state and the *Z*-dimer is derived both from the singlet (S_1) state (e.g., the excited "van der Waals dimer") and the T_1 state, though mainly from the former. However, the low Φ_{ST} values reported previously[26,27] imply that the triplet state would not be efficiently produced on direct irradiation. For example, Dunsbach and Schmidt have determined Φ_{ST} to be 0.00 ± 0.02 in toluene by employing photoacoustic calorimetry.[6] Samanta and Fessenden failed to observe transient absorption due to the T_1 state on nanosecond laser flash photolysis of ACN in cyclohexane (10^{-3}−10^{-2} M), but observed it with a lifetime of 1−5 μs on excitation in the presence of heavy-atom-containing solvents, such as iodoethane and bromoethane, or sensitizers, such as benzil and pyrene.[26] They detected emission on 266 nm laser excitation of ACN and assigned this not to phosphorescence of the T_1 state, but to fluorescence from a populated higher singlet (S_2) state.[27]

If the *E*-dimer is produced from the T_1 state, the question then arises, how is the *E*-dimer formed on direct irradiation of ACN in the absence of heavy atom solvents or sensitizers? A plausible possibility is participation of the T_1 state produced by intersystem crossing from the S_1 state competitively with its reaction and rapid nonradiative decay. As described above, Φ_{ST} is very low and thus difficult to determine accurately. However, intersystem crossing could occur competitively with the reaction from the short-lived S_1 state under conditions where the latter is considerably suppressed. Thus, to corroborate participation of the T_1 state, irradiation of a sufficiently dilute solution should be effective, since the reaction rate from the S_1 state could then be slow enough to compete with intersystem crossing. Cowan and coworkers employed [ACN] higher than 0.3 M to facilitate isolation of the isomeric dimers and unconverted ACN after irradiation.[19,20,22−24] From the singlet lifetime, τ_S, of 0.35 ns,[5] the rate constant for the intersystem crossing, k_{ST}, can be estimated to be 3×10^7 s^{-1}, assuming Φ_{ST} is 10^{-2}. If the rate constant for dimerization from the S_1 state, k_r^S, is assumed to be 10^9 M^{-1} s^{-1}, under the conditions used by Cowan et al. ([ACN] = 0.3−1.2 M), k_r^S[ACN] is greater than 3×10^8 s^{-1}, which is at least 10 times greater than k_{ST}. Obviously, at such a high [ACN], the singlet ACN would be trapped by ground state ACN or decay radiationlessly before it could convert to the T_1 state. Therefore, [ACN] > 0.3 M seems to be inappropriate to examine the role of the T_1 state under direct irradiation.

The aim of our study was to elucidate the mechanism of the photodimerization of ACN under direct irradiation, especially to quantify the role of the pathways from the singlet and the triplet states, by examining the reaction in solution over a wide range of concentrations. We also examined the effects of a triplet sensitizer, a triplet quencher, and heavy-atom-containing solvents. Herein, we present evidence of the involvement of the triplet (T_1) state, generated in low quantum yield from the singlet (S_1) state by intersystem crossing, in the dimerization of ACN under irradiation at high dilution.

Scheme 1

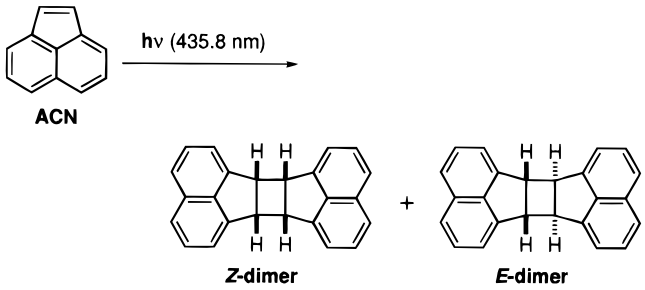

Results

Direct Irradiation of ACN in Various Solvents. The *Z*- and *E*-dimers of ACN show absorption at wavelengths shorter than 370 nm. Irradiation of these dimers with 365 nm light leads to gradual photoreversion to ACN. In order to avoid this complication (Scheme 1), monochromatic 435.8 nm light was employed for irradiation of ACN. Irradiation of ACN (2.0×10^{-4}−2.0 M) in various solvents at 435.8 nm led to stoichimetric conversion of the consumed ACN into the two dimers without any detectable byproduct, based on examination of the reaction mixture by ^{1}H-NMR and GC.

Figure 1 plots the quantum yields of the dimerization, Φ_R, determined by means of ^{1}H-NMR measurement of disappearance of ACN, against [ACN] in 1,2-dichloroethane (DCE), acetonitrile (AN), cyclohexane (CH), benzene (BZ), methanol (MeOH), and *N*,*N*-dimethylformamide (DMF) over a wide range of [ACN]. Φ_R increased to a plateau level with increase of [ACN]. In the low [ACN] region, Φ_R was highest in DCE among the solvents used, but with increase of [ACN] the difference of Φ_R between the solvents was reduced, and finally in the highest concentration region (close to the maximum solubility in the solvents at 25 °C) Φ_R showed little difference among the solvents. Φ_R in MeOH could not be measured at higher concentration than 5.7×10^{-1} M ACN because of low solubility in this solvent.

Figure 2 plots reciprocal quantum yield, Φ_R^{-1}, against reciprocal concentration of ACN, $[ACN]^{-1}$. The plots are biphasic, with smaller slopes at low [ACN], that is, the high $[ACN]^{-1}$ region (Figure 2a), and larger ones at high [ACN], that is, the low $[ACN]^{-1}$ region (Figure 2b). The linear relationship in the high [ACN] region in Figure 2b gives slopes of 2.18, 3.84, and 4.56 M and intercepts of 4.82, 3.50, and 2.60 with the correlation coefficient (*r*) of 0.984, 0.996, and 0.998 in DCE, AN, and CH, respectively. In a similar manner, from the nearly linear relationship in the low [ACN] region in Figure 2a, the slopes are 0.760, 2.32, and 2.54 M, and intercepts are 6.25, 32.4 and 29.3 with *r* of 0.998, 0.993, and 0.979 in DCE, AN, and CH, respectively.

Figure 3 shows the ratio of the *Z*- to the *E*-dimer, *Z*/*E* ratio, determined by ^{1}H-NMR, as a function of [ACN]. The *Z*/*E* ratio increases nearly linearly with increase of [ACN], with larger slopes in polar solvents such as AN and DMF, but there is little sensitive to [ACN] in DCE.

(22) Cowan, D. O.; Drisco, R. L. *J. Am. Chem. Soc.* **1970**, *92*, 6281−6285.
(23) Cowan, D. O.; Kozier, J. C. *J. Am. Chem. Soc.* **1974**, *96*, 1229−1230.
(24) Cowan, D. O.; Kozier, J. C. *J. Am. Chem. Soc.* **1975**, *97*, 249−254.
(25) Koser, G. F.; Liu, V-S. *J. Org. Chem.* **1978**, *43*, 478−481.
(26) Samanta, A.; Fessenden, R. W. *J. Phys. Chem.* **1989**, *93*, 5823−5827.
(27) Samanta, A. *J. Am. Chem. Soc.* **1991**, *113*, 7427−7429.

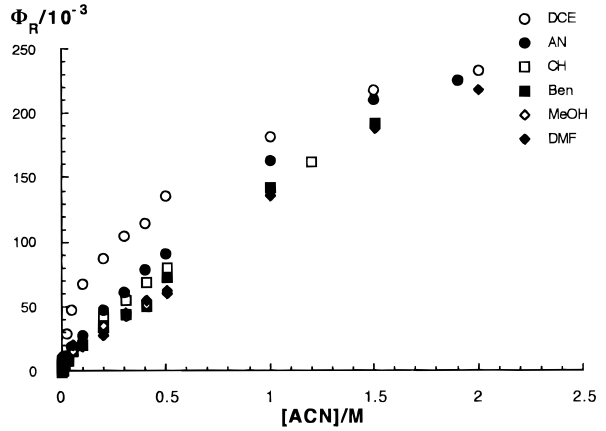

Figure 1. Plots of the quantum yield of ACN, Φ_R, against the concentration of ACN, [ACN], in dichloroethane (DCE), acetonitrile (AN), cyclohexane (CH), benzene (Ben), methanol (MeOH), and *N*,*N*-dimethylformamide (DMF).

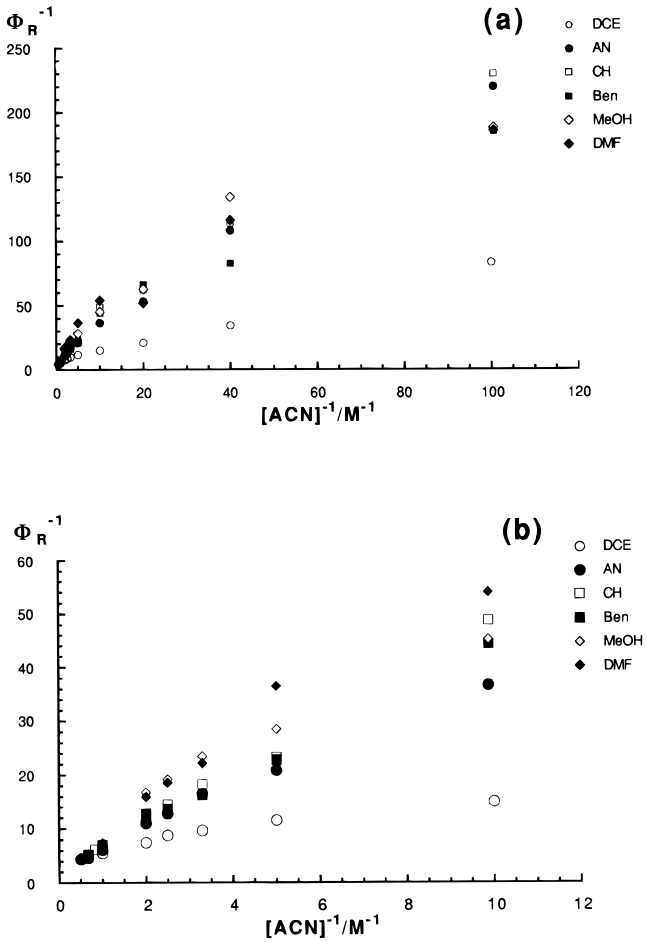

Figure 2. (a) Plots of the reciprocal of quantum yield for photodimerization of ACN, Φ_R^{-1}, versus reciprocal concentration of ACN, $[ACN]^{-1}$. (b) Expanded plots in the high [ACN] region in part a.

Irradiation in the Presence of DBE, a Heavy-Atom-Containing Solvent. To examine the effect of a heavy-atom-containing solvent on the photodimerization, ACN (1.0×10^{-3} M) was irradiated at 435.8 nm in DCE, AN, and CH in the presence of various amounts of 1,2-dibromoethane (DBE). Figure 4 plots Φ_R^{DBE} of the dimerization against added DBE. The Φ_R^{DBE} values increased rapidly as the fraction of DBE was increased from 0 to 2.5 vol %. For example, on irradiation in 2.5 vol % of DBE, Φ_R^{DBE} in AN jumped 6-fold from 4.2×10^{-4} to 2.5×10^{-3}. Similar drastic increases were observed in other solvents. On further increase of the fraction of DBE, however, Φ_R^{DBE} approached the same plateau value.

On the other hand, as Figure 5 shows, the *Z*/*E* ratio was insensitive to addition of DBE in DCE and CH, and remained at 0.6 and 0.4, respectively. In AN, however, the *Z*/*E* ratio decreased from 1.7 in 0 vol % to 0.5 in 100% DBE.

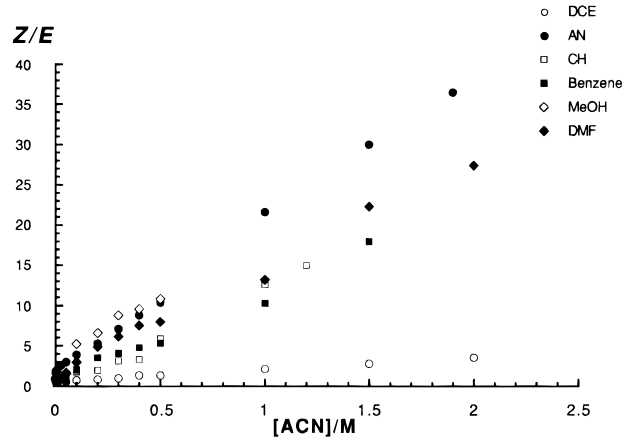

Figure 3. Plots of the *Z*/*E* ratio of photodimerization of ACN against [ACN].

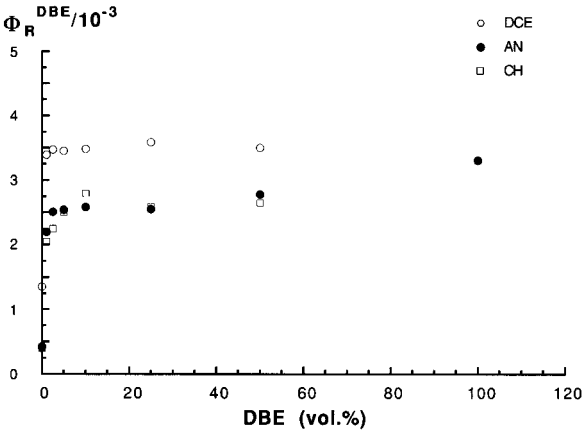

Figure 4. Plots of the quantum yield of photodimerization of ACN against vol % of 1,2-dibromoethane (DBE) in DCE, AN, and CH.

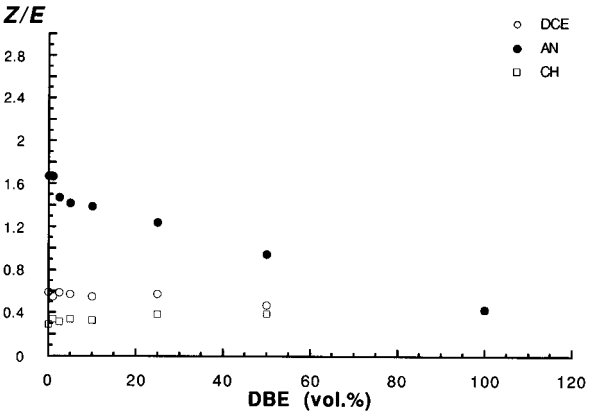

Figure 5. Plots of the *Z*/*E* ratio of photodimerization of ACN against vol % of DBE in DCE (open circles), AN (closed circles), and CH (open squares).

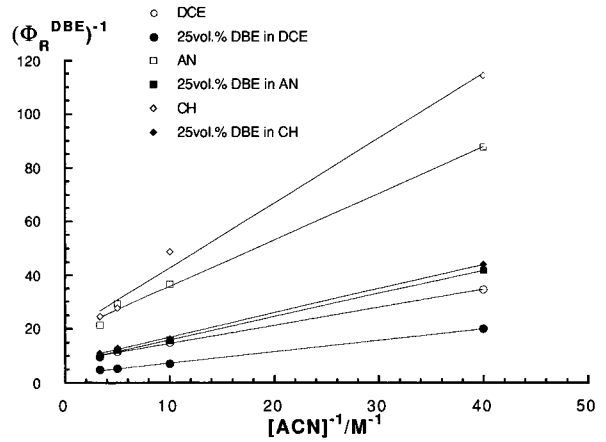

Figure 6. Plots of the reciprocal of quantum yield for photodimerization of ACN, Φ_R^{-1}, versus reciprocal concentration of ACN, $[ACN]^{-1}$, in the presence of 25 vol % DBE (closed symbols) and in the absence of DBE (open symbols) in DCE, AN, and CH.

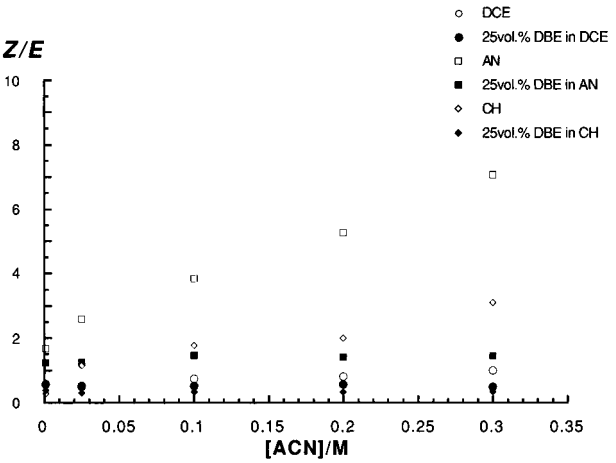

Figure 7. Plots of Z/E ratio versus [ACN] in the presence of 25 vol % DBE (closed symbols) and in the absence of DBE (open symbols) in DCE, AN, and CH.

To see the effect of [ACN] on Φ_R in the presence of DBE, ACN of varying concentration was irradiated in the presence of 25 vol % DBE in DCE, AN, and CH. The Φ_R^{DBE} increased with increase of [ACN] and finally attained a plateau, as observed in the direct irradiation in the absence of DBE (Figure 2). Among these solvents, Φ_R^{DBE} was highest in DCE over the whole range of [ACN] examined. Plots of $(\Phi_R^{DBE})^{-1}$ versus $[ACN]^{-1}$, as presented in Figure 6, show single slope values of 0.420, 0.864, and 0.903 M, and intercepts of 3.16, 7.25, and 7.88 with r of 0.999, 0.999, and 0.999 in DCE, AN, and CH, respectively. The Z/E ratios take nearly constant, small values, 0.6 in DCE, 1.3 in AN, and 0.5 in CH, over the whole range of [ACN] (Figure 7).

Effect of a triplet sensitizer. Rose Bengal and Eosin-Y were previously used to sensitize dimerization of ACN under irradiation with light of longer wavelength than 510 nm in methanol (0.66 M), giving the dimers with the Z/E ratio of 0.5.[20] The triplet energy of ACN (E_T) was estimated as 192.5−196.6 kJ mol^{-1} from the rate constants for quenching of the transient absorption of the triplet ACN, generated in the presence of iodoethane, by quenchers with various E_T values.[26] To examine the behavior of the T_1 state, the quantum yields of sensitized dimerization of ACN, Φ_R^{sens}, were determined on irradiation at 546.1 nm in the presence of Eosin-Y (E_T = 195.8 kJ mol^{-1}), which has a large absorption coefficient in this wavelength region ($\epsilon_{546\ nm}$ = 2600). The energy transfer from the triplet state of Eosin-Y to ACN is expected to proceed efficiently, since it might be slightly exothermic or thermoneutral. Mixed solvents containing 10 vol % ethanol were used to increase the solubility of Eosin-Y.

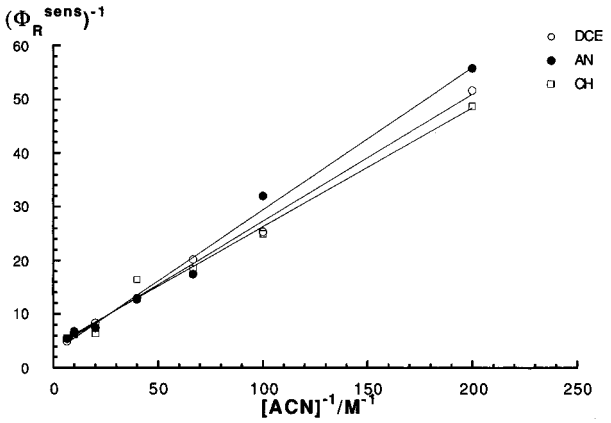

Figure 8. Plots of $(\Phi_R^{sens})^{-1}$ versus $[ACN]^{-1}$ in DCE, AN, and CH.

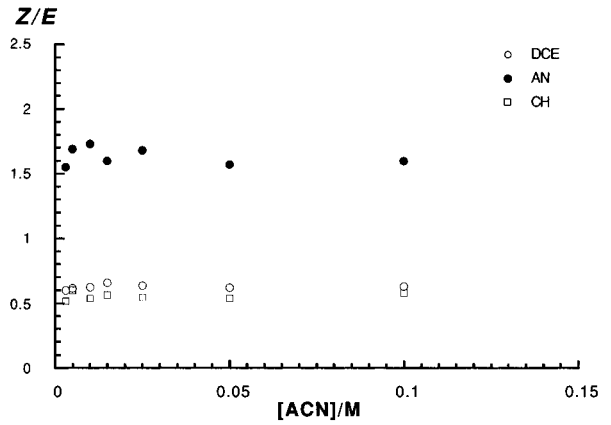

Figure 9. Plots of Z/E ratio versus [ACN] in the photodimerization of ACN sensitized by Eosin-Y in DCE, AN, and CH.

Irradiation of Eosin-Y in the presence of ACN afforded the two dimers more effectively than direct irradiation, without formation of byproducts. Relation between Φ_R^{sens} and [ACN] in DCE, AN, and CH containing 10 vol % ethanol shows curves increasing with increase of [ACN], similar to those in the case of direct irradiation. Plots of $(\Phi_R^{sens})^{-1}$ against $[ACN]^{-1}$ (Figure 8) gave straight lines for each solvent. It is noteworthy that these straight lines have very similar slopes to each other, such as 0.237, 0.265, and 0.223 M with intercepts of 3.56, 2.87, and 4.02 with r of 0.998, 0.995, and 0.994 in DCE, AN, and CH, respectively. The Z/E ratios remained essentially constant over the entire range of [ACN], being 0.65, 1.60, and 0.58 in DCE, AN, and CH, respectively (Figure 9), which are very close to the values seen on direct irradiation in the presence of DBE (Figure 7).

Quenching by Ferrocene. In order to estimate quantitatively the role of the T_1 state in the photodimerization, irradiation of ACN was carried out in the presence of a triplet quencher. Ferrocene (Fc), whose E_T value is 159 kJ mol^{-1},[28] is expected to quench triplet ACN with a diffusion-controlled rate constant. As shown in Table 1, addition of small amounts of ferrocene dramatically depressed the photodimerization of [ACN] (1.0×10^{-2} M). For example, on addition of 1.0×10^{-3} M Fc in

Table 1. Quantum Yield (Φ_R) and *Z/E* Ratio for the Photodimerization of ACN in the Presence and Absence of Ferrocene (Fc)[a]

solvent	[Fc]/M	$\Phi_R/10^{-3}$	*Z*/E
DCE	0	29.0	0.508
DCE	1.0×10^{-4}	14.0	1.02
DCE	1.0×10^{-3}	4.27	5.20
DCE	5.0×10^{-3}	2.80	11.3
DCE	1.0×10^{-2}	2.55	41.4
AN	0	11.4	2.14
AN	1.0×10^{-4}	3.26	11.7
AN	1.0×10^{-3}	2.44	33.0
AN	5.0×10^{-3}	2.24	
AN	1.0×10^{-2}	2.28	
CH	0	8.74	0.958
CH	1.0×10^{-4}	5.30	2.01
CH	1.0×10^{-3}	2.59	6.68
CH	5.0×10^{-3}	2.30	18.5
CH	1.0×10^{-2}	2.20	43.6

[a] Irradiation of 2.5×10^{-2} M ACN solution at 435.8 nm.

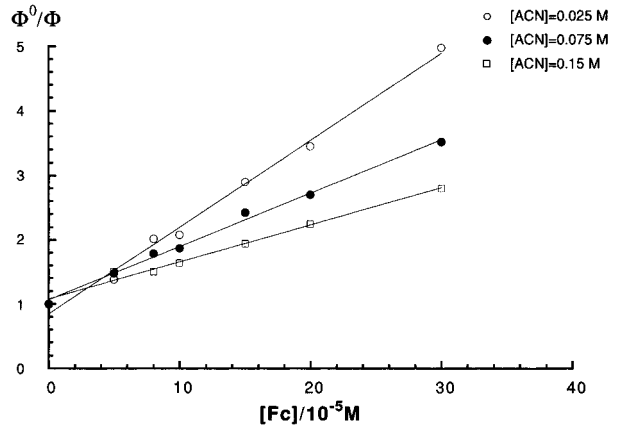

Figure 10. Typical Stern−Volmer plots for quenching of the photodimerization of ACN by ferrocene (Fc).

AN, Φ_R decreased from 1.1×10^{-2} to 2.4×10^{-3}. Further increase of Fc, however, did not completely suppress the reaction but gave a nearly constant value of 2.3×10^{-3} in the presence of 1.0×10^{-2} M Fc. The *Z*/*E* ratios increased with the decrease of Φ_R. Thus, addition of 1.0×10^{-3} M Fc increased the *Z*/*E* ratio from 2.14 to 33.0, and addition of 1.0×10^{-2} M Fc suppressed the formation of even a trace amount of the *E*-dimer, as examined by ^{1}H-NMR or by GC. Similar results were observed in DCE and CH.

To estimate the triplet lifetime, τ_T, and the rate constant for the reaction of the triplet ACN with ground state ACN, k_r^T, several fixed concentrations of ACN were irradiated in 25 vol % of DBE in the presence of varying concentrations of Fc, and the relative quantum yield in the presence of Fc, Φ_R^{Fc}, to that in the absence of Fc, Φ_R^0, were determined. Figure 10 presents typical Stern−Volmer plots for 2.5×10^{-2}, 7.5×10^{-2}, and 1.5×10^{-1} M [ACN] in DCE. The plots afforded a linear relationship for each [ACN]. Similar results were obtained for quenching in AN and in CH.

Discussion

Dimerization from the Singlet State. Cowan and Drisco observed that Φ_R linearly increases with [ACN] (concentration: >0.3 M) in both BZ and CH.[20] The present determination of Φ_R over a wide range of [ACN], especially in the lower [ACN] region (2.0×10^{-4}−5.0×10^{-2} M), reveals a clear biphasic dependence of Φ_R^{-1} on $[ACN]^{-1}$ (Figure 2); this indicates that independent mechanisms dominate the dimerization in the lower and higher concentration regions. The mechanism of the photodimerization of ACN presented in Scheme 2 is consistent with our results. Thus, the singlet excited state, S_1, due to its very short lifetime, predominantly reacts with ACN in the higher [ACN] region; on the other hand, the T_1 state formed with low efficiency through intersystem crossing from the S_1 state has a longer lifetime and plays the dominant role in the reaction with ACN in the lower [ACN] region.

Scheme 2

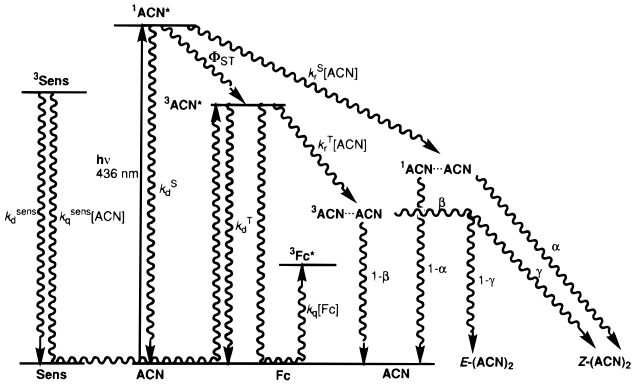

The singlet ACN undergoes either nonradiative decay with a rate constant, k_d^S, corresponding to the reciprocal lifetime of the S_1 state, $(\tau_S)^{-1}$, or addition to ground state ACN with a rate constant of k_r^S to give an intermediate. The resulting intermediate collapses to the *Z*-dimer with an efficiency of α, competing with reversion to two ground state ACN molecules. When Fc nearly completely quenches the triplet ACN, the yield of the *E*-dimer is suppressed (Table 1). Therefore, it is clear that the dimerization from the S_1 state exclusively leads to the *Z*-dimer. Though we found no evidence for formation of the proposed "van der Waals dimer",[17] the singlet ACN might interact with ground state ACN to give an intermediate, such as a nonradiative excimer with a favorable close orientation of the two aromatic rings, that would lead only to the *Z*-dimer without affording the *E*-dimer.

According to Scheme 2, Φ_R is composed of contributions from the S_1 and the T_1 states (eq 1). As mentioned above, Φ_R^S and Φ_R^T correspond to Φ_R in the higher and lower [ACN] regions, respectively. The quantum yield from the S_1 state, Φ_R^S, is represented by eq 2, from which the reciprocal quantum yield, $(\Phi_R^S)^{-1}$, is derived as given in eq 3.

$$\Phi_R = \Phi_R^S + \Phi_R^T \tag{1}$$

$$\Phi_R^S = \frac{k_r^S[ACN]\alpha}{k_r^S[ACN] + \tau_s^{-1}} = \frac{k_r^S\tau_S[ACN]\alpha}{1 + k_r^S\tau_S[ACN]} \tag{2}$$

$$\frac{1}{\Phi_R^S} = \frac{1}{\alpha}\left(1 + \frac{1}{k_r^S\tau_S[ACN]}\right) \tag{3}$$

Thus, $(\Phi_R^S)^{-1}$ linearly increases with $[ACN]^{-1}$ with an intercept of α^{-1} and a slope of $(\alpha k_r^S\tau_S)^{-1}$. The observed linear relationship in the higher [ACN] region in Figure

(28) Murov, S. L.; Carmichael, I.; Hug, G. L. *Handbook of Photochemistry*, 2nd ed.; Marcel Decker, Inc.: New York, 1993; pp 58.
(29) Lessing, H. E.; Richardt, D.; von Jena, A. *Mol. Struct.* **1982**, *84*, 281−292.

Table 2. Kinetic Data for the Photodimerization of ACN from the Singlet State

	DCE	AN	CH
a	0.257	0.286	0.385
$k_r^S\tau_S/M^{-1}$	2.21	0.991	0.570
$k_r^S/M^{-1}\ s^{-1}$ [a]	6.3×10^9	2.6×10^9	1.6×10^9

[a] Estimated from $\tau_S = 3.6 \times 10^{-10}$ s.

2b gives α as 0.207, 0.286, and 0.385 and $k_r^S\tau_S$ as 2.21, 0.911, and 0.570 M^{-1} in DCE, AN, and CH, respectively, as summarized in Table 2. In each solvent, α is close to one-third. This means that in the final step in dimerization from the S_1 state, the intermediate collapses to the *Z*-dimer with an efficiency of $\alpha \cong 0.3$ and reverts to the starting ACN with an efficiency of $1 - \alpha \cong 0.7$, regardless of the solvents. $k_r^S\tau_S$ is obtained as the ratio of the intercept to the slope in Figure 2b. Substitution of the τ_S value in CH (3.5×10^{-10} s [5]) into the estimated $k_r^S\tau_S$ gives k_r^S of 6.3×10^9, 2.6×10^9, and 1.6×10^9 M^{-1} s^{-1} in DCE, AN, and CH, respectively, and those values are close to the diffusion-controlled rate constant in each solvent. These estimated data are included in Table 2.

Dimerization from the Triplet State. (a) Direct Irradiation. The S_1 state of ACN is converted into the T_1 state with an efficiency of Φ_{ST}, and this state either deactivates with a lifetime, τ_T, or reacts with ground state ACN with a rate constant of k_r^T to give an intermediate. The resulting intermediate collapses to the *Z*- or the *E*-dimer with an efficiency of β, competing with dissociation to two ground state ACN. The quantum yield for dimerization from the T_1 state, Φ_R^T, is expressed by eq 4. At low [ACN] (<1.0×10^{-2} M), where the T_1 state predominantly reacts with ACN, $k_r^S\tau_S$[ACN] (Table 2) in the denominator of the first term of eq 4 is much smaller than unity (Table 2) and can be neglected. Therefore, the reciprocal Φ_R^T, that is $(\Phi_R^T)^{-1}$, increases linearly with $[ACN]^{-1}$ at low [ACN], as in eq 5.

$$\Phi_R^T = \frac{k_{ST}}{k_r^S[ACN] + \tau_S^{-1}} \frac{k_r^T[ACN]\beta}{k_r^T[ACN] + \tau_T^{-1}} = \frac{\Phi_{ST}}{1 + k_r^S\tau_S[ACN]} \frac{k_r^T\tau_T[ACN]\beta}{1 + k_r^T\tau_T[ACN]} \quad (4)$$

$$\frac{1}{\Phi_R^T} = \frac{1}{\beta\Phi_{ST}}\left(1 + \frac{1}{k_r^T\tau_T[ACN]}\right) \quad (5)$$

From the linear relation between $(\Phi_R^T)^{-1}$ and $[ACN]^{-1}$ in the low [ACN] domain under direct irradiation in Figure 2a, one can obtain $(\beta\Phi_{ST})^{-1}$ as an intercept and $(\beta\Phi_{ST})^{-1}(k_r^T\tau_T)^{-1}$ as a slope. The $\beta\Phi_{ST}$ values are extrapolated as 0.155, 0.0309, and 0.0341, and the $k_r^T\tau_T$ values are obtained as 8.22, 13.9, and 11.5 M^{-1} in DCE, AN, and CH, respectively. These data are listed in Table 3 together with other data concerning the T_1 state.

On the basis of the α, $k_r^S\tau_S$, $\beta\Phi_{ST}$, and $k_r^T\tau_T$ values obtained above, Φ_R^S and Φ_R^T at various [ACN] were calculated according to eqs 3 and 5, and the ratio of the calculated Φ_R^S/Φ_R^T to [ACN] is depicted in Figure 11. It is clear that in the low concentration region the T_1 state dominates the reaction and the contribution from the S_1 state is negligible; however, with increase of [ACN], the reaction from the S_1 state is increasingly favored and finally becomes the sole reaction pathway.

(b) Irradiation in the Presence of DBE. In the photodimerization of ACN in the presence of 25 vol % DBE, the observed linear relation with a single slope in the plots of $(\Phi_R^{DBE})^{-1}$ versus $[ACN]^{-1}$ in Figure 6 indicates that only one excited state, the T_1 state, participates in the reaction. Quantum yields for this reaction, Φ_R^{DBE}, are given by replacing the first term of eq 4 by the quantum yield for intersystem crossing in the presence of DBE, Φ_{ST}^{DBE}, and replacing τ_T in the second term by the triplet lifetime in the presence of DBE, τ_T^{DBE}, affording eq 6. In 25 vol % DBE, the T_1 state will be populated by $S_0 \rightarrow T_1$ absorption enhanced by the heavy atom effect of DBE.

Table 3. Quantum Yields for Intersystem Crossing of ACN, in the Presence or Absence of DBE, and Kinetic Data for the Photodimerization of ACN from the Singlet State

	DCE	AN	CH
$\beta\Phi_{ST}$ [a]	0.155	0.0309	0.034
$\beta\Phi_{ST}^{DBE}$ [b]	0.316	0.138	0.127
β [b]	0.85	1.05	0.75
Φ_{ST}	0.18	0.029	0.045
Φ_{ST}^{DBE}	0.37	0.13	0.17
$k_r^T\tau_T/M^{-1}$ [a]	8.22	13.9	11.5
$k_r^T\tau_T/M^{-1}$ [b]	14.9	10.8	18.0
$k_r^T\tau_T/M^{-1}$ [c]	7.52	8.43	8.76
$k_r^T\tau_T/M^{-1}$ [d]	6.24	3.98	11.6
$k_r^T/M^{-1}\ s^{-1}$ [d]	2.13×10^6	1.78×10^6	2.94×10^6
τ_T/s [d]	2.93×10^{-6}	2.24×10^{-6}	3.94×10^{-6}
γ [d]	0.337	0.618	0.361
γ [b]	0.393	0.615	0.367

[a] Determined by direct irradiation at low [ACN] in the absence of additives. [b] Determined by Eosin-Y-sensitized reaction on irradiation at 546.1 nm. [c] Determined by direct irradiation in the presence of 25 vol % of DBE. [d] Determined by quenching with Fc.

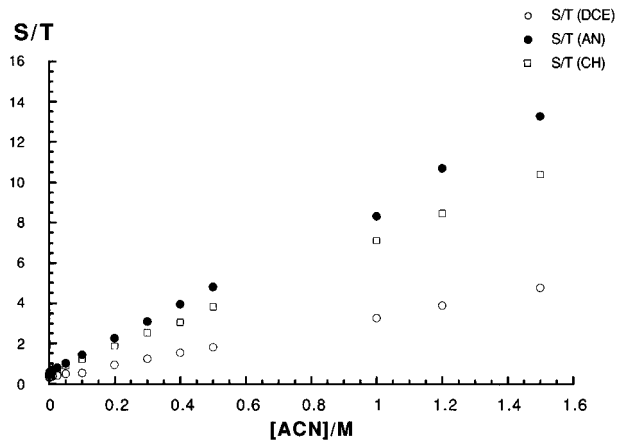

Figure 11. Ratio of quantum yield from the singlet state and that from the triplet state, S/T, calculated according to eqs 2 and 4, against [ACN] in DCE, AN, and CH.

$$\Phi_R^{DBE} = \Phi_{ST}^{DBE}\frac{k_r^T\tau_T^{DBE}[ACN]\beta}{1 + k_r^T\tau_T^{DBE}[ACN]} \quad (6)$$

Equation 7 shows that $(\Phi_R^{DBE})^{-1}$ linearly increases with $[ACN]^{-1}$ with an intercept of $(\beta\Phi_{ST}^{DBE})^{-1}$ and a slope of $(\beta\Phi_{ST}^{DBE})^{-1}(k_r^T\tau_T^{DBE})^{-1}$. Using the slopes and intercepts of the straight lines in Figure 6, $\beta\Phi_{ST}^{DBE}$ and $k_r^T\tau_T^{DBE}$ are obtained (Table 3).

$$\frac{1}{\Phi_R^{DBE}} = \frac{1}{\beta\Phi_{ST}^{DBE}}\left(1 + \frac{1}{k_r^T\tau_T^{DBE}[ACN]}\right) \quad (7)$$

(c) Sensitization by Eosin-Y. The β values can be estimated by employing the sensitizer Eosin-Y. The

sensitization processes are depicted in Scheme 2, where k_q^{sens} and k_d^{sens} are rate constants for energy transfer from the triplet sensitizer to ACN and for decay of the triplet state. The quantum yields for sensitized dimerization, Φ_R^{sens}, is given by eq 8, where Φ_{ST}^{sens} represents the quantum yield for intersystem crossing of the sensitizer; this has a value of 0.33[29] for Eosin-Y.

$$\Phi_R^{sens} = \Phi_{ST}^{sens} \frac{k_q^{sens}[ACN]}{k_q^{sens}[ACN] + k_d^{sens}} \frac{k_r^T[ACN]\beta}{k_r^T[ACN] + k_d^T} \quad (8)$$

Because the triplet energy of Eosin-Y is slightly higher than or comparable with that of ACN, the energy transfer process from the triplet sensitizer to ACN is expected to proceed much more efficiently than the decay of the triplet sensitizer ($k_q^{sens}[ACN] \gg k_d^{sens}$). Hence, eq 8 can be simplified as follows.

$$\Phi_R^{sens} = \Phi_{ST}^{sens} \frac{k_r^T[ACN]\beta}{k_r^T[ACN] + k_d^T} \quad (9)$$

Applying eq 10 to the observed linear relation of $(\Phi_R^{sens})^{-1}$ against $[ACN]^{-1}$ (Figure 8), one can obtain β and $k_r^T\tau_T$ values, which are included in Table 3. The obtained β values are 0.85 in DCE, 1.05 in AN, and 0.75 in CH, which are larger than the α values (≅0.3 in each solvent) in the S_1 state (Table 2). Thus, the intermediate from the T_1 state collapses more efficiently to the dimer than does that from the S_1 state.

$$\frac{1}{\Phi_R^{sens}} = \frac{1}{\beta\Phi_{ST}^{sens}}\left(1 + \frac{1}{k_r^T\tau_T[ACN]}\right) \quad (10)$$

(d) Efficiency of Intersystem Crossing. By using β values obtained above, Φ_{ST} and Φ_{ST}^{DBE} values can be estimated from $\beta\Phi_{ST}$ and $\beta\Phi_{ST}^{DBE}$, as listed in Table 3. The Φ_{ST} values thus obtained are small in AN and CH (both 0.03), but fairly large in DCE (0.19). The above estimation of Φ_{ST} in AN and CH is in contrast to the report by Samanta and Fessenden, who did not observe transient absorption of the T_1 state on excitation of ACN ([ACN]: 10^{-3}−10^{-2} M) in BZ or in CH with a 337.1 or 355 nm pulsed laser, but observed it on excitation in the presence of heavy-atom-containing solvents.[26] However, the present result in CH is compatible with the Φ_{ST} determined by means of photoacoustic calorimetry (0.00 ± 0.02) in toluene by Dunsbach and Schmidt.[6] This reported low efficiency might be negligible if it were determined in not-very-dilute solution, where dimerization can take place from the S_1 state. The more dilute the solution, the more significant the intersystem crossing becomes. Higher Φ_R values on direct irradiation of ACN in DCE than in CH and AN can be ascribed to the larger Φ_{ST} value in DCE.

Larger values for Φ_{ST}^{DBE}, on the order of 0.1 in each solvent, show that in DBE the dimerization takes place predominantly from the T_1 state. Thus, in CH, for example, k_{ST} is estimated to be 4.8×10^8 s^{-1}, which is 3 times larger than the pseudo-first-order rate constant from the S_1 state, $k_r^S[ACN]$, of 1.6×10^8 s^{-1} at high [ACN] of 1.0×10^{-1} M.

It should be noted that in DCE Φ_{ST} is more than 4 times larger and Φ_{ST}^{DBE} is more than 2 times larger than those in AN and CH. This obvious acceleration of intersystem crossing in DCE may be attributed to the spin−orbit coupling between the chlorine atom in DCE and singlet ACN.[30]

The ratio of the probability of intersystem crossing by one atom (P_1) to that by another atom (P_2) is expressed as follows, since P is generally proportional to the square of the spin−orbit coupling parameter, ζ:[30]

$$\frac{P_1}{P_2} = \frac{\zeta_1^2}{\zeta_2^2} \quad (11)$$

Cowan and Drisco observed dramatic heavy-atom effects on the efficiency of photodimerization of ACN in solvents containing iodine and bromine atoms, but not chlorine. They found a good correlation corresponding to eq 11 for the plot of the chemical yield of the *E*-dimer against ζ and concluded that the effects of iodinated and brominated solvents result from the spin−orbit coupling of these heavy atoms.[22] Using the values for ζ of 587 for chlorine and 2460 cm^{-1} for bromine,[31] $(P_{DBE})/(P_{DCE})$ is calculated to be 17.56, which is, however, 8 times larger than the observed $(\Phi_{ST}^{DBE})/\Phi_{ST}^{DCE})$ value of 2.06.

(e) Product Distribution from the Triplet State. In the presence of a sufficient concentration of Fc, ACN triplet is completely quenched by Fc. Under this condition all of the dimer is necessarily produced by way of the S_1 state and only the *Z*-dimer is formed. Therefore, using the data in Table 1, according to eq 12, one can

$$\frac{Z}{E} = \frac{\Phi_R^{Fc} + \gamma\Phi_R^0}{(1-\gamma)\Phi_R^0} \quad (12)$$

calculate from the observed Z/E values the proportion for the *Z*-dimer produced from the T_1 state, γ, as 0.337, 0.618, and 0.361 in DCE, AN, and CH, respectively (Table 3).

Cowan and Drisco reported that the triplet ACN affords a larger amount of the *E*-dimer accompanied by a smaller amount of the *Z*-dimer, and the ratio depends on the nature of the solvent employed; the γ values were estimated as 0.30, 0.26, and 0.20 in MeOH, BZ, and CH, respectively.[20] Also, under Eosin-Y sensitization, only the triplet state is generated and reacts with ACN to give a certain ratio of the *Z*- and *E*-dimer in each solvent (Figure 9); the γ values obtained are also included in Table 3. The γ values obtained from the quenching by Fc and by triplet sensitizer agree fairly well with each other. The present γ values in DCE and CH are similar to those reported in CH.

As described above, in DCE and CH the T_1 state gives a larger amount of the *E*-dimer than the Z-dimer ($\gamma < 0.5$); however, in AN the T_1 state gives a larger amount of the *Z*-dimer ($\gamma > 0.5$) than the *E*-dimer. This finding rationalizes the higher Z/E ratio observed in AN, even at low [ACN], than those in other solvents. Thus, in 1.0×10^{-3} M ACN without additives, the observed Z/E ratio, 1.56 in AN, is considerably higher than that of 0.51 in DCE or 0.47 in CH (Figure 3). The Z/E ratios calculated using the above γ values are 0.42 for DCE, 1.51 for AN, and 0.46 for CH, which are in satisfactory agreement with the observed values under low [ACN] conditions. Therefore, the observed predominance of the *Z*-dimer at low [ACN] in AN is attributable not to the participation

(30) EI-Sayed, M. A. *Acc. Chem. Res.* **1968**, *1*, 8.

(31) Murov, S. L.; Carmichael, I.; Hug, G. L. *Handbook of Photochemistry*, 2nd ed.; Marcel Decker, Inc.: New York, 1993; pp 339.

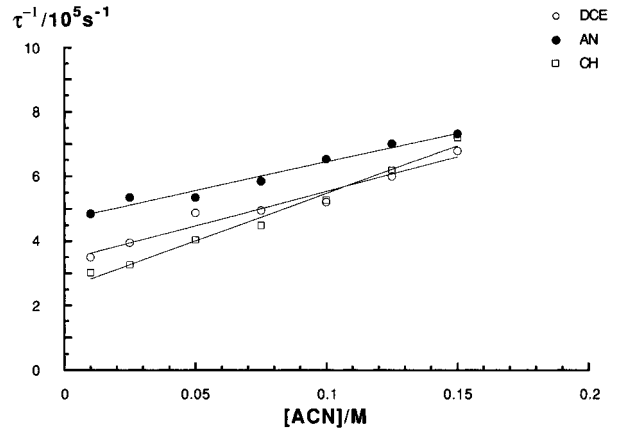

Figure 12. Plots of reciprocal of triplet lifetime (τ^{-1}) determined by means of a Stern−Volmer quenching experiment employing ferrocene versus [ACN].

of the S_1 state, but to a high γ value from the T_1 state in AN. The results of the irradiation in AN containing a varying fraction of DBE clearly support this (Figure 5). The *Z*/*E* ratio decreased from 1.53 in 0 vol % to 0.65 in 100 vol % of DBE. This dramatic decrease of the *Z*/*E* ratio with the increase of DBE originates from the difference of γ value between AN and DBE. In DCE and CH, whose γ values are close to that of DBE, the *Z*/*E* ratio varied only slightly with varying fraction of DBE.

(f) Kinetic Parameters from the Triplet State. The observed linear relationship in Stern−Volmer plots (Figure 10) indicates that Fc quenches the triplet ACN with a rate constant k_q competing with ground state ACN, as shown in Scheme 2. Then the quantum yield in the presence of Fc is expressed by the following eq.

$$\Phi_R^{Fc} = \Phi_{ST}\frac{k_r^T[ACN]}{\tau_T^{-1} + k_r^T[ACN] + k_q[Fc]}\beta \qquad (13)$$

The ratio of the quantum yields at a given ACN concentration in the absence of Fc, Φ_R^0, to that in the presence of Fc, Φ_R^{Fc}, is represented by eq 14, where $\tau_T^{[ACN]}$ stands for the triplet lifetime at that [ACN], as expressed by eq 15.

$$\frac{\Phi_R^0}{\Phi_R^{Fc}} = 1 + k_q\tau_T^{[ACN]}[Fc] \qquad (14)$$

$$(\tau_T^{[ACN]})^{-1} = \tau_T^{-1} + k_r^T[ACN] \qquad (15)$$

Equation 14 fits the observed relationship in Figure 10, with an intercept very close to unity, as expected. The slope corresponds to $k_q\tau_T^{[ACN]}$. By dividing the slopes by the k_q values, which are assumed to be diffusion-controlled rate constants, 4.4×10^9, 1.1×10^{10}, and 3.8×10^9 M^{-1} s^{-1} in DCE, AN and CH, respectively,[32] $\tau_T^{[ACN]}$ can be estimated. By varying [ACN], $\tau_T^{[ACN]}$ at the respective [ACN] can be determined. The $(\tau_T^{[ACN]})^{-1}$ obtained is plotted against [ACN] in Figure 12. This indicates that $(\tau_T^{[ACN]})^{-1}$ increases linearly with increase of [ACN], with k_r^T as a slope and $(\tau_T)^{-1}$ as an intercept. The observed values in DCE, AN, and CH are 2.13×10^6, 1.78×10^6 and 2.94×10^6 M^{-1} s^{-1} for k_r^T and 2.93×10^{-6}, 2.24×10^{-6}, and 3.94×10^{-6} s for τ_T with *r* of 0.978, 0.986, and 0.993, respectively (Table 3).

The obtained τ_T values are 2−4 μs, and are 10 000 times larger than τ_S. The long lifetime of the T_1 state enables it to react with ground state ACN in spite of the low efficiency of its formation via intersystem crossing from the S_1 state. The above τ_T values are comparable to those (1−5 μs) reported by Samanta and Fessenden, measured from the transient absorption of the T_1 state in various concentrations of iodoethane or bromoethane in CH.[26]

The values of $k_r^T\tau_T$, the product of k_r^T and τ_T, each determined by quenching experiments employing Fc, are 6.24, 3.98, and 11.6 M^{-1} in DCE, AN, and CH, respectively, as included in Table 3. These values are similar in magnitude to the $k_r^T\tau_T$ values obtained from the reciprocal plots of $(\Phi_R^{DBE})^{-1}$ against $[ACN]^{-1}$ (Figure 6) in the case of irradiation in the presence of DBE, the plots of $(\Phi_R^{sens})^{-1}$ versus [ACN] for the sensitization reactions (Figure 8), and the plots in the dilute concentration region under direct irradiation (Figure 2a). The conformity among the results of the above four independent methods is convincing evidence for participation of the T_1 state in the photodimerization of ACN in dilute solution under direct irradiation (Scheme 2). The slightly smaller $k_r^T\tau_T^{DBE}$ values than $k_r^T\tau_T$ values may be attributed to the shorter triplet lifetime of ACN in the presence of DBE.

The $k_r^S\tau_S$ or $k_r^T\tau_T$ values represent the ratio of addition of the S_1 or T_1 state to ground state ACN (when [ACN] = 1 M) to deactivation from the S_1 (T_1) state. The 10 times larger value for $k_r^T\tau_T$ (≅10 M^{-1}) than for $k_r^S\tau_S$ (≅1 M^{-1}) shows that, in the low [ACN] region, the latter process is not effective and the former process in the T_1 state plays a predominant role. This, together with the larger values for β than for α, is responsible for higher quantum yields of the dimerization in the presence of DBE or Eosin-Y. For example, quantum yields for the dimerization ([ACN] = 2.5×10^{-2} M) were increased from 9.3×10^{-3} in the absence of additives to 2.4×10^{-2} and 7.7×10^{-2} in the presence of 25 vol % of DBE and in the case of sensitization by Eosin-Y, respectively.

Dependence of the *Z*/*E* Ratio on [ACN]. Further support for the mechanism of this photodimerization in Scheme 2 is derived from analysis of the *Z*/*E* ratio versus [ACN] relationship (Figure 3). According to this scheme, the *Z*/*E* ratio upon direct irradiation of ACN in the absence of additives is expressed in eq 16 using γ value, Φ_R^S, and Φ_R^T. Plots of the *Z*/*E* ratio against [ACN] should give a straight line with a slope of $(k_r^S\tau_S\alpha)\{(1-\gamma)\beta\Phi_{ST}\}$ and an intercept of $\gamma/(1-\gamma) + (k_r^S\tau_S\alpha)\{(1-\gamma)\beta\Phi_{ST}k_r^T\tau_T\}$.

$$\frac{Z}{E} = \frac{\Phi_R^S + \gamma\Phi_R^T}{(1-\gamma)\Phi_R^S} = \frac{\gamma}{1-\gamma} + \frac{k_r^S\tau_S\alpha}{(1-\gamma)\beta\Phi_{ST}k_r^T\tau_T} + \frac{k_r^S\tau_S\alpha[ACN]}{(1-\gamma)\beta\Phi_{ST}} \qquad (16)$$

As expected from eq 16, in each solvent the *Z*/*E* ratio gives a straight line (Figure 3). For DCE, AN, and CH, the slopes and intercepts were compared with $(k_r^S\tau_S\alpha)/\{(1-\gamma)\beta\Phi_{ST}\}$ and $\gamma/(1-\gamma) + (k_r^S\tau_S\alpha)/\{(1-\gamma)\beta\Phi_{ST}k_r^S\tau_T\}$ estimated from the values in Tables 2 and 3, and the results are summarized in Table 4. The slopes mostly agree rather well with $(k_r^S\tau_S\alpha)\{(1-\gamma)\beta\Phi_{ST}\}$. Similarly,

(32) Wagner, P. J.; Kochevar, I. *J. Am. Chem. Soc.* **1968**, *90*, 2232−2238.

Table 4. Observed and Calculated Slopes and Intercepts in the Linear Relationship between [ACN] and *Z/E* ratio on Direct Irradiation of ACN

	DCE	AN	CH
slope[a]	1.50	18.6	11.9
$k_r^S\tau_S\alpha/\{(1-\gamma)\beta\Phi_{ST}\}$[b]	6.04	21.9	10.2
intercept[a]	0.55	1.83	0.205
$\gamma/(1-\gamma)+k_r^S\tau_S\alpha/\{(1-\gamma)\beta\Phi_{ST}k_r^T\tau_T\}$[b]	1.05	3.62	1.14

[a] From Figure 3. [b] Calculated according to eq 16.

the intercepts agree well with $\gamma/(1-\gamma)+(k_r^S\tau_S\alpha)\{(1-\gamma)\beta\Phi_{ST}k_r^S\tau_T\}$, except for that in DCE, 1.50, which is less than the $(k_r^S\tau_S\alpha)\{(1-\gamma)\beta\Phi_{ST}\}$ value of 6.04. These agreements substantiate the validity of the mechanism shown in Scheme 2.

Conclusions

We have examined in detail the mechanism of the photodimerization of ACN, particularly the role of the S_1 and T_1 states in formation of the *Z*- and *E*-dimers. On irradiation of ACN with 435.8 nm light in DCE, AN, CH, BZ, MeOH, and DMF over a wide concentration range (2.0×10^{-4}–2.0 M), both the Φ_R and the *Z*/*E* ratio increased with increase of [ACN], but not linearly. Plots of $(\Phi_R)^{-1}$ against $[ACN]^{-1}$ are biphasic, showing predominant participation of the S_1 and T_1 states in the higher and lower [ACN] regions, respectively. Direct irradiation of ACN in the presence of DBE, a heavy-atom-containing solvent, and sensitization with Eosin-Y (irradiated at 546.1 nm) led to more efficient dimerization than direct irradiation in the absence of additives and afforded the two dimers in ratios that depended on the solvent: rich in the *E*-dimer in DCE and CH, but rich in the *Z*-dimer in AN. On the other hand, irradiation in the presence of Fc, a triplet quencher, resulted in less efficient dimerization than direct irradiation without Fc and exclusively afforded the *Z*-dimer. The above facts have clarified the mechanism of the photodimerization of ACN. Thus, in concentrated solution, the S_1 state reacts with the ground state of ACN before intersystem crossing to the T_1 state can occur, affording exclusively the *Z*-dimer. On the other hand, in dilute solution, the S_1 state crosses over to the T_1 state, though with very low quantum yield except in DCE, before reaction with the ground state of ACN can occur, due to the very short lifetime of the S_1 state, and the resultant T_1 state acts on ACN to give a mixture of the *Z*- and *E*-dimers. Very low but significant quantum yields for intersystem crossing, Φ_{ST}, 0.029 in AN and 0.045 in CH, were unambiguously demonstrated, which is consistent with an important role of the T_1 state at very low concentration. This finding is in contrast to a previous report that the absorption of the T_1 state was observed on laser excitation of ACN in the presence of heavy-atom-containing solvents, but was not observed in the absence of additives in CH.[26] The *Z*/*E* ratio produced from the T_1 state, γ, determined by sensitization with Eosin-Y, depends on the solvent used, with preference for the *E*-dimer in DCE (0.337) and in CH (0.361), but for the *Z*-dimer in AN (0.618). The γ values are close to those estimated from the quenching experiment with ferrocene. Significant participation of the T_1 state in the lower [ACN] region under direct irradiation is confirmed by the similarity of $\beta\Phi_{ST}$ and $k_r^T\tau_T$ values estimated from direct irradiation in dilute solution of ACN with those from irradiation in the presence of DBE or sensitization with Eosin-Y. The 10 000-fold longer lifetime of the T_1 state of 10^{-6} s (estimated by Stern–Volmer quenching with Fc) than that of the S_1 state of 10^{-10} s, together with the larger β values (estimated from sensitization with Eosin-Y) than α values in each solvent, contributes to the higher Φ_R from the T_1 state than the S_1 state at low [ACN].

Experimental Section

General. Common analytical instruments (melting point, ^{1}H-NMR, UV, EI-MS, GC, flash column chromatography, and thin layer chromatography) and the merry-go-round apparatus for photolysis are the same as in our previous papers.[33,34] Microanalyses were carried out in the microanalytical laboratory of our school.

Materials and Solvents. Acenaphthylene (Tokyo Kasei) was purified by recrystallization of the picrate at least three times from benzene and ethanol.[20] Dissociation of the picrate by aqueous ammonia followed by extraction with *n*-hexane gave light yellow prisms, mp 93.0 °C (lit.[24] mp 92–93 °C). This material was analytically pure, and no trace of impurity (such as acenaphthene) was detected either by ^{1}H-NMR or by GC. Fc (Wako) and Eosin-Y (Wako) were recrystallized from ethanol. Potassium ferrioxalate was synthesized according to the literature.[35]

Spectral-grade DCE, AN, CH, MeOH, and BZ (Dojin) and infinity-grade DMF (Wako) were used for photodimerization as supplied. DBE (Tokyo Kasei) was purified according the literature method.[36]

Isolation of 435.8 and 546.1 nm Light. Monochromatic light of 435.8 nm was extracted by passing the light from a high-pressure mercury lamp through a colored glass filter (HOYA L-42, which corresponds to Corning 3389) and a solution filter (path length: 1 cm) which contained 44.0 g of copper sulfate, 75.0 g of sodium nitrite, and 60 mL of 25% aqueous ammonia in 300 mL of water.[37] Similarly, 546.1 nm monochromatic light was obtained by using a combination of a colored glass filter (HOYA, Y-50, which corresponds to Corning 3486) and a solution filter (path length: 1 cm) containing 50.0 g of neodymium nitrate, 13.3 g of copper chloride(II), and 18 g of calcium chloride in 300 mL of water.[38] Transmittance of both of the solution filters was unchanged after 24 h of irradiation.

Preparation of the *Z*- and *E*-Dimers of ACN. The authentic *Z*- and *E*-dimers of ACN were prepared by large-scale irradiation at 435.8 nm of ACN in DCE solution and isolated by flash column chromatography (eluent: *n*-hexane–dichloromethane). *Z*-Dimer: recrystallized from dichloromethane–hexane as colorless cubes; mp 233.5–234.5 °C (lit.[20] mp 231–233.5 °C). EI-MS: m/e 304 (M^+). ^{1}H-NMR: δ 7.19 (d, 4H, J = 8.0, 1.0 Hz), 7.14 (dd, 4H, J = 8.0, 7.3 Hz), 7.01 (dd, 4H, J = 7.3, 1.0 Hz), 4.84 (s, 4H). Anal. Calcd for $C_{24}H_{16}$: C 94.70, H 5.30; Found: C 94.50, H 5.44. *E*-Dimer: recrystallized from hot benzene as colorless needles; mp 304.0–306.0 °C (dec) in a sealed tube (lit.[20] mp 305–307 °C). EI-MS: *m/e* 304 (M^+). ^{1}H-NMR: δ 7.74 (dd, 4H, J = 8.1, 1.0 Hz), 7.60 (dd, 4H, J = 8.1, 7.9 Hz), 7.01 (dd, 4H, J = 7.9, 1.0 Hz), 4.10 (s, 4H). Anal. Calcd for $C_{24}H_{16}$: C 94.70, H 5.30; Found: C 94.51, H 5.34.

Quantum Yields for Photodimerization of ACN on Direct Irradiation. Quantum yields for the reaction were determined according to the usual procedure with ferrioxalate actinometry.[39] Solutions of ACN in 10 or 50 mL Pyrex test tubes, 2.0 mm in thickness, were degassed to about 10^{-3} Torr

(33) Haga, N.; Kuriyama, Y.; Takayanagi, H.; Ogura, H.; Tokumaru, K. *Photochem. Photobiol.* **1995**, *61*, 557–562.
(34) Haga, N.; Takayanagi, H. *J. Org. Chem.* **1996**, *61*, 735–745.
(35) Kuhn, H. J.; Braslavsky, S. E.; Schmidt, R. *Pure. Appl. Chem.* **1989**, *61*, 188–210.
(36) Perrin, D. D.; Armarego, W. L. F. *Purification of Laboratory Chemicals*, 3rd ed.; Pergamon Press, 1988; pp 141.
(37) Calvert, J. G.; Pitts, J. N., Jr. *Photochemistry*; John Wiley & Sons, Inc.: New York, 1966; pp 737–738.
(38) Calvert, J. G.; Pitts, J. N., Jr. *Photochemistry*; John Wiley & Sons, Inc.: New York, 1966; pp 739–740.

in three freeze−pump−thaw cycles, then the tubes were sealed and irradiated with 435.8 nm light in parallel in a merry-go-round apparatus at 25 ± 2 °C. Irradiation time, which depends on the solvent, [ACN], and the presence of DBE, Eosin-Y, and Fc, was controlled to keep the conversion low. After irradiation, the solvent was removed under reduced pressure. The resulting mixture was dissolved in dichloromethane and subjected to GC analyses. Conditions of measurement were as follows: column, Ultra ALLOY$^+$-1 (HT) (FRONTIER LAB.); column length, 30 m; column diameter, 0.25 mm; film thickness, 0.25 mm, injection port, 200 °C; detector, 300 °C; column temperature, initially 170 °C, elevated at 17 °C/min to 270 °C. Retention times (min) were 4.13 for ACN, 15.08 for the *Z*-dimer, and 20.05 for the *E*-dimer. Yields of recovered ACN and the dimers were determined from calibration curves. For each of the samples, three or four measurements were performed and averaged.

When precise quantification of the products by GC was unsuccessful because of low conversion or low yield of the *E*-dimer, ^{1}H-NMR analyses were employed. The residual mixture after irradiation was dissolved in $CDCl_3$ without isolation. The signals of δ 7.08 (s) for ACN, 4.84 (s) for the *Z*-dimer, and 4.10 (s) for the *E*-dimer were used to determine relative yields of recovered ACN and the two products. No peaks arising from other products were detected.

Quantum Yields for Sensitized Photodimerization of ACN. Mixed solvents containing 10 vol % ethanol were used for the sensitized reaction. ACN solution containing Eosin-Y (1.0×10^{-4} M) in Pyrex test tubes was degassed by means of freeze−pump−thaw cycles and irradiated with 546.1 nm light in parallel in a merry-go-round apparatus. Conversion of ACN was kept low. Quantum flux values were measured by ferrioxalate actinometry, whose quantum yield at 546.1 nm is 0.15.[40] Conversion of ACN and yields of the dimers were determined by employing ^{1}H-NMR analyses as described above. Traces of byproducts were found in the sensitized reaction.

Quenching by Fc. ACN solution (2.5×10^{-2} M) containing an appropriate concentration of Fc in Pyrex test tubes was degassed by means of freeze−pump−thaw cycles and irradiated with 435.8 nm light in a merry-go-round apparatus using ferrioxalate actinometry. Quantification of ACN and the two dimers was performed by means of ^{1}H-NMR described above.

For relative quantum yields, ACN solutions containing 25 vol % DBE in the absence and in the presence of various concentrations of Fc were simultaneously irradiated in a merry-go-round apparatus. The resulting mixtures were quantified by ^{1}H-NMR.

Acknowledgment. This work was partly supported by a Grant-in Aid for Scientific Research (No. 07740506, NH) from the Ministry of Education, Science, and Culture, Japan.

Supporting Information Available: Plots of the quantum yield of photodimerization of ACN against [ACN] in the presence of 25 vol % DBE and plots of the quantum yield of photodimerization of ACN against [ACN] in the presence of Eosin-Y in DCE, AN, and CH (2 pages). This material is contained in libraries on microfiche, immediately follows this article in the microfilm version of the journal, and can be ordered from the ACS; see any current masthead page for ordering information.

Registry Numbers Provided by the Authors. ACN, 208-96-8; *Z*-dimer, 15065-28-8; *E*-dimer, 14620-98-5.

JO962397O

(39) Hatchard, C. G.; Parker, C. A. *Proc. R. Soc. London, Ser. A* **1956**, *235A*, 518−36.

(40) Murov, S. L.; Carmichael, I.; Hug, G. L., *Handbook of Photochemistry*, 2nd ed.; Marcel Decker, Inc.: New York, 1993; pp 303.